

Small angle neutron scattering study of disordered and crystalline iron nanoparticle assemblies

D.F. Farrell^a, Y. Ijiri^b, C.V. Kelly^b, J.A. Borchers^c, J.J. Rhyne^d, Y. Ding^e, S.A. Majetich^{e,*}

^aPhysics Department, University College London, London WC1E 7HN, UK

^bPhysics and Astronomy Department, Oberlin College, Oberlin, OH 44074, USA

^cNIST Center for Neutron Research, National Institute of Standards and Technology, Gaithersburg, MD 20899, USA

^dLos Alamos National Laboratory, Los Alamos, NM 87545, USA

^ePhysics Department, Carnegie Mellon University, Pittsburgh, PA 15213-3890, USA

Available online 3 March 2006

Abstract

Monodisperse surfactant-coated iron nanoparticles are used to form both disordered nanoparticle assemblies and ordered face-centered cubic nanoparticle crystals. The structural order is probed by small angle X-ray scattering, and the magnetic scattering is studied using small angle neutron scattering. The magnetic scattering corresponding to different length scales is interpreted in terms of collective correlations among the particles within the assemblies.

© 2006 Elsevier B.V. All rights reserved.

PACS: 75.50.Tt; 61.12.Ex; 78.67.Bf; 78.70.Ck

Keywords: Magnetic nanoparticle; Small angle neutron scattering; Small angle X-ray scattering; Self-assembled array; Nanoparticle crystal

1. Introduction

Monodisperse magnetic nanoparticles in self-assembled structures are of technological importance for possible data storage media [1], and are a model system for the study of magnetic interactions in artificial ferromagnets [2–4]. In the nanoparticles proposed for data storage media, the main experimental goal has been to generate the high coercivity $L1_0$ phase of FePt in an ordered array, and interactions between particles are undesirable.

In contrast, with strongly interacting Fe or Co nanoparticles, the structure within the assembly plays a significant role in the collective magnetic behavior [2–4]. Compared with exchange interactions within a bulk ferromagnet, the magnetostatic interactions between particles are weak, but it is possible to have a purely dipolar ferromagnet [5–7]. There have been numerous experimental studies of magnetostatic effects in concentrated dispersions of monodisperse particles [2–4,8–14]. A typical concen-

trated sample is a self-assembled array with nearly close-packed, surfactant-coated particles and a volume fraction of between 25% and 45%. The upper limit to the volume fraction is limited only by the thickness of the particle coating and the size of the particles.

Little is known about the details of the spin arrangements within these assemblies. Dilute frozen ferrofluids have been shown to behave like dipolar spin glasses [15]. As the nanoparticle concentration increases and the interactions strengthen, theories predict that face-centered cubic (3D) and hexagonal (2D) assemblies will have a ferromagnetic ground state at $T = 0$ K. [16] At elevated temperatures, or with less perfectly ordered assemblies, the length scale of magnetic ordering will presumably be reduced, but so far there has been little quantitative data.

The most common signatures of collective behavior in magnetometry measurements involve a broadening of the zero field-cooled magnetization curve and a shift in its peak to higher temperature. The coercivity and remanence show more complex changes. The most sensitive magnetic properties to magnetostatic interactions are the time-dependent magnetic relaxation and the frequency-dependent

*Corresponding author. Tel.: +1 412 268 3105; fax: +1 412 681 0648.
E-mail address: sm70@andrew.cmu.edu (S.A. Majetich).

susceptibility [4]. Because small angle neutron scattering (SANS) is sensitive to magnetic moment orientations on a very short time scale ($\sim 10^{-11}$ s) [17], and because it is sensitive to the length scale of magnetic ordering, it offers a unique tool to address important questions regarding the spin structures within interacting nanoparticle assemblies. Here we describe our SANS investigation of iron nanoparticles that consist of either disordered arrays or ordered, face-centered cubic (FCC) crystals.

2. Experimental methods

The synthesis of Fe nanoparticles has been described in detail elsewhere [4,18,19]. The particles used in this study were made in a low boiling point solvent, decalin, rather than dioctyl ether. This leads to particles with less crystalline internal structure due to dissolved carbon and a lower specific magnetization ($\sigma_s \sim 120$ emu/g). Nanoparticle crystals were grown by slowly diffusing a poorly coordinating solvent into a stable dispersion of Fe nanoparticles in toluene using the method of Talpin et al. [20]. Comparison samples with different degrees of order were made by growing the nanoparticle crystals over a four-week period [2,3], and by rapidly evaporating the solvent to create a thick composite with glassy ordering. The glassy sample was formed from 8.6 ± 0.7 nm particles, and the nanoparticle crystal samples were made from the same batch of 8.5 ± 0.7 nm particles. Both samples had similar coercivities (~ 200 Oe) and remanence ratios ($M_r/M_s \sim 0.10$ – 0.14) at 10 K. Compared with the SANS nanoparticle crystals, the small angle X-ray scattering (SAXS) sample was grown with a higher 2-propanol:toluene volume ratio (1.8:1 versus 1:1).

The nanoparticle assemblies were characterized magnetically by SQUID magnetometry at low temperatures. Transmission electron microscopy was used to determine the particle size, while SAXS and SANS were used to find the length scale of structural ordering in the nanoparticle crystals, which were too thick to be electron transparent. Because neutrons are also sensitive to magnetic moments, SANS was used to determine the length scale for magnetic ordering in the nanoparticle crystals. SAXS measurements were taken at the Brookhaven National Synchrotron Light Source beam line X21B using transmission geometry, with an X-ray wavelength of 0.1211 nm. SANS data were taken at the NG-7 spectrometer at the NIST Center for Neutron Research. Details of the SANS measurements are provided elsewhere [18].

3. Results and discussion

The intensity versus scattering vector determined from SAXS is sensitive to the higher charge density of the Fe cores. A sample of 8.5 nm particles grown by nanoparticle crystallization shows all the expected peaks of an FCC crystal, with a lattice spacing of 16.5 nm and an average edge-to-edge interparticle spacing of 3.2 nm (Fig. 1). In

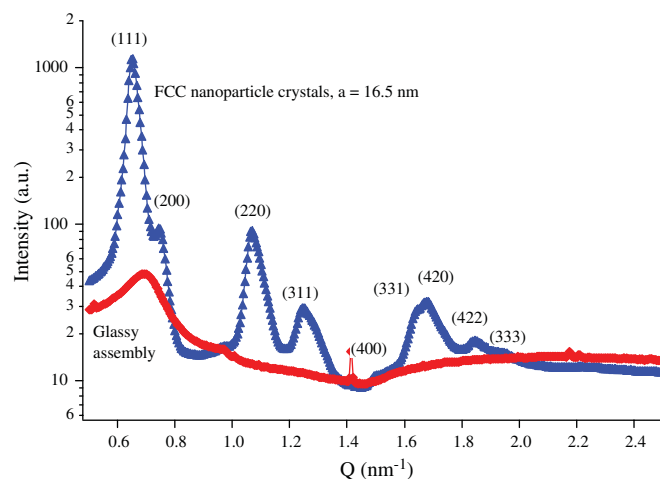


Fig. 1. Angle-averaged SAXS intensity as a function of Q , for rapidly quenched assemblies and nanoparticle crystals that have a FCC lattice structure. Both samples were made from 8.5 nm Fe nanoparticles. The wavelength was 0.1211 nm.

contrast, the sample grown by rapid solvent evaporation shows only one clear peak, which is near, but above, the position corresponding to the close-packed (1 1 1) reflection for the crystal. In the more dilute particle assembly, a scattering peak corresponding to the inverse minimal distance of approach is observed, as has been reported earlier [21]. As the particles begin to form more ordered arrangements and constructive interference between planes of particles becomes more significant, this peak shifts to lower angles.

SANS is sensitive to both nuclear and magnetic structure of the sample and thus can detect variations in the latter that arise from changes in temperature or application of a magnetic field. Compared with the angular range shown in the SAXS data of Fig. 1, the range of scattering vectors $Q = 4\pi \sin \theta / \lambda$ is much smaller. SANS is therefore less useful for the determination of the *structural* order of these nanoparticle assemblies. However, the crystalline sample shows evidence of the (1 1 1) peak at 0.80 nm^{-1} and the (2 2 0) peak at 1.27 nm^{-1} , which are consistent with a FCC structure with spacing ~ 13.6 nm (Fig. 2(a)). This corresponds to 8.5 nm particles with an edge-to-edge spacing of 1.1 nm, the same separation obtained in previous SAXS measurements on nanoparticle crystals [2,3]. The reason for the larger separation found with the SAXS sample is not clear, but could arise from differences in the amount of surfactant coating the particle surfaces.

Unlike the SAXS intensities, the SANS signal shows an increase in intensity with lower Q or θ . Fig. 2(b) shows that most, though not all, of this low Q intensity for the glassy sample disappears when a large magnetic field is applied at both 5 and 150 K, indicating that this signal is magnetic in origin. Above the blocking temperature of the nanoparticles, the magnetic signal due to correlations should be negligible. While 150 K exceeds the blocking temperature for SQUID magnetometry measurements on these particles

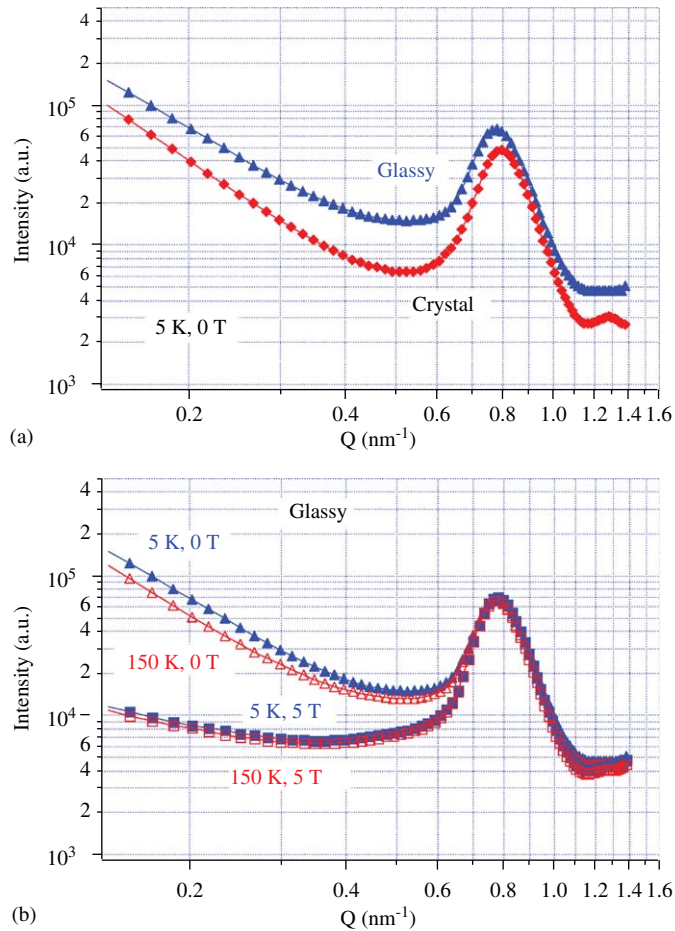


Fig. 2. (a) SANS intensity versus scattering vector Q for a nanoparticle crystal and a glassy assembly of Fe nanoparticles. (b) SANS intensity versus scattering vector Q for the glassy assembly of Fig. 2(a), at different temperatures and applied fields. All data are angle averaged.

[4], the measurement time is much shorter for neutron scattering, and the particles may still be effectively blocked for the SANS results of Fig. 2(b). In addition, magnetic signal from individual, now uncorrelated particles may be observed.

Magnetic correlations within the nanoparticle assemblies are highlighted by subtracting data taken at 5 T. This approach also assumes that most of the magnetic moments are aligned parallel to the 5 T field and do not contribute to magnetic scattering. At the diffraction peak, differences in intensity $\Delta I = I(0 \text{ T}) - I(5 \text{ T})$ depend on the angle θ between the scattering vector Q and the applied field H (Fig. 3(a)). From neutron scattering selection rules [18], the high-field magnetic intensity at the diffraction peak will be minimal for $\theta = 0^\circ$ and 180° if the particle moments are aligned with the field. Fig. 3(a) shows that the angular dependence is $\Delta I \propto \sin^2\theta$, as expected when moments align parallel to the applied field. We note, however, that the oscillation in the nanoparticle crystals is sharper than that in the glassy assembly. Previous work has shown that the spins in the shells of partially oxidized particles can become canted perpendicular to the applied field and have

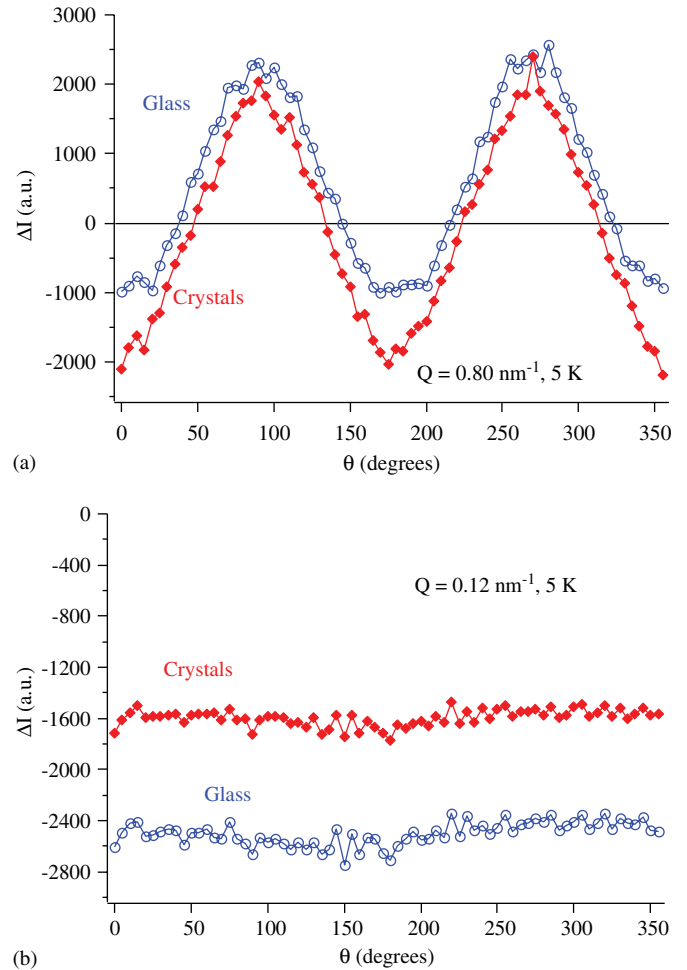


Fig. 3. Angular dependence of intensity difference $\Delta I = I(0 \text{ T}) - I(5 \text{ T})$ at 5 K, for the nanoparticle crystals and glassy assemblies. (a) Average at $Q = 0.80 \text{ nm}^{-1}$ (the diffraction peak), corresponding to a length scale of 7.85 nm. (b) Average at $Q = 0.12 \text{ nm}^{-1}$, corresponding to a length scale of ~ 53 nm.

increased rather than decreased scattering perpendicular to Q at the diffraction peak position [18]. The particles discussed here were minimally oxidized, but can still be expected to have roughly 0.5 nm of iron oxide on their surfaces, which appears to be insufficient to support magnetic order.

Judging by the field dependence in Fig. 2(b), the lower Q region has a significant magnetic component. Since these Q values correspond to length scales larger than a single particle, these data contain information about the interparticle magnetic interactions within the assemblies. Many groups have observed sizeable magnetic scattering at low values of Q for nanoparticles [17,21,22] and nanocrystalline materials [23–27], but the interpretation of its cause and its functional form is still under debate. Isolated monodisperse particles should have a spin correlation function proportional to $\exp(-\kappa_{\text{pt}}r)$, where r is a distance comparable to the particle radius and κ_{pt} is the inverse of the intraparticle magnetic correlation length. The Fourier transform of the correlation function leads to a Lorentzian-squared

dependence of the intensity on Q . An empirical Lorentzian factor has been used to account for the additional intensity at low Q [17,21]:

$$I_{\text{mag}}(Q) = \frac{A}{(Q^2 + \kappa_{\text{pt}}^2)^2} + \frac{B}{Q^2 + \kappa_{\text{corr}}^2}. \quad (1)$$

Here the length scale of the correlations between particles $L_{\text{corr}} = 1/\kappa_{\text{corr}}$. Using this approach, our data for the glassy sample at 5K would suggest correlated regions over 100 nm, in analogy to multi-grain correlations reported in nanocrystalline alloys [24,27]. However, this picture may be too simplistic for the current data, as the quality of fits to such a functional form is imperfect. While the particles are monodisperse at the 5–10% variation level, some scattering from small clusters of coalesced nanoparticles might distort the low Q signal.

In addition, the combination of a Lorentzian-squared and Lorentzian SANS lineshape has been interpreted in amorphous TbFe₂ as arising from a combination of scattering from static regions plus dynamical scattering, respectively [28]. The lower Q magnetic scattering from our Fe nanoparticle assemblies could be dynamic in origin as well. The fluctuations could include both spin waves within the particles plus collective fluctuations in the moments of multiple coupled particles.

Magnetic X-ray circular dichroism (XMCD) measurements on 9 nm Co nanoparticle assemblies have also shown field-dependent reductions in scattering at Q values below the diffraction peak [13]. The results were interpreted in terms of an antiferromagnetic orientation of neighboring particle moments, which would effectively double the lattice spacing. In our case, antiferromagnetic correlations in the SANS data would appear as a magnetic peak centered near $Q = 0.40 \text{ nm}^{-1}$. Since the scattering in this region is broad, antiferromagnetic correlations, if present, are short ranged.

Instead, in our SANS data, magnetic scattering intensity in 0T persists over length scales corresponding to many particle diameters. However, as shown in Fig. 3(b) for $Q = 0.12 \text{ nm}^{-1}$, away from the diffraction peak, $\Delta I = I(0\text{T}) - I(5\text{T})$ does not have much angular dependence for either the crystal or for the glassy assembly. For the crystal sample, this result is consistent with an interpretation involving interparticle correlations in 0T. The application of a large magnetic field should dramatically increase the magnetic correlation length among the particles, and the magnetic scattering depicted at $Q = 0.12 \text{ nm}^{-1}$ in 5T should go to zero. For the glassy sample, this interpretation is less clear because some of the scattering in this low Q region might be expected to originate from individual particles that are not in well-formed arrays. A dependence of $\Delta I \propto \sin^2\theta$ is expected to some degree. While it is likely that the low Q scattering for both the glassy and crystal samples involve long-range interparticle magnetic correlations, it is still an open question.

4. Conclusions

Monodisperse Fe nanoparticles in crystalline and glass-like assemblies were studied by small angle X-ray and neutron scattering. SAXS was useful for characterizing the degree of structural order within an assembly, for determining the average interparticle spacing, and for identifying possible lattice structures. SANS revealed fewer details about the lattice structure but provided a measurement of a magnetic length scale that may be associated with long-range interparticle interactions.

There have been numerous efforts using SANS to determine a magnetic correlation length scale in nanostructured materials. In our nanoparticle assemblies that should have only magnetostatic interactions, we see some evidence of long-range magnetic correlations, based on the decrease in the magnetic scattering intensity at low Q values with the application of a magnetic field and the angle dependent data at different Q values. However, a cleaner signature is necessary to obtain more quantitative information.

In future work we will apply these SANS techniques to higher moment particles to determine whether it is possible to observe magnetically stable regions within an assembly.

Acknowledgments

This work was supported by the National Science Foundation grants CTS-0227645 and ECS-0304453 (S.A.M.), the American Chemical Society Petroleum Research Fund grants PRF 40049-B5M (Y.I.) and PRF 37578-AC5 (S.A.M.), a Research Corporation grant CC5820 (Y.I.) and a University of Missouri Research Board Grant (J.J.R.). This work utilized facilities supported in part by the National Science Foundation under agreement DMR-9986442. We thank L. Yang of the National Synchrotron Light Source at Brookhaven National Laboratory for assistance with the SAXS measurements.

References

- [1] S. Sun, C.B. Murray, D. Weller, L. Folks, A. Moser, *Science* 287 (2000) 1989.
- [2] D. Farrell, Y. Ding, S.A. Majetich, C. Sanchez-Hanke, C.C. Kao, *J. Appl. Phys.* 95 (2004) 6636.
- [3] D. Farrell, Y. Cheng, Y. Ding, S. Yamamuro, C. Sanchez-Hanke, C.-C. Kao, S.A. Majetich, *J. Magn. Magn. Mater.* 282 (2004) 1.
- [4] D. Farrell, Y. Cheng, R.W. McCallum, M. Sachan, S.A. Majetich, *J. Phys. Chem. B* 109 (2005) 13409.
- [5] J.M. Luttinger, L. Tisza, *Phys. Rev.* 70 (1946) 954.
- [6] G. Mukhopadhyay, P. Apell, M. Hanson, *J. Magn. Magn. Mater.* 203 (1999) 286.
- [7] J.F. Fernandez, J.J. Alonso, *Phys. Rev. B* 62 (2000) 53.
- [8] V.F. Puentes, K.M. Krishnan, P. Alivisatos, *Appl. Phys. Lett.* 78 (2001) 2187.
- [9] G.A. Held, G. Grinstein, H. Doyle, S. Sun, C.B. Murray, *Phys. Rev. B* 64 (2001) 012408.
- [10] P. Poddar, T. Telem-Shafir, T. Fried, G. Markovich, *Phys. Rev. B* 66 (2002) 060403.

- [11] V. Russier, C. Petit, J. Legrand, M.P. Pileni, *Phys. Rev. B* 62 (2000) 3910.
- [12] M. Giersig, M. Hilgendorff, *J. Phys. D: Appl. Phys.* 32 (1999) L111.
- [13] J.B. Kortright, O. Hellwig, K. Chesnel, S. Sun, E.E. Fullerton, *Phys. Rev. B* 71 (2005) 012402.
- [14] P. Poddar, J.L. Wilson, H. Srikanth, D.F. Farrell, S.A. Majetich, *Phys. Rev. B* 68 (2003) 214409.
- [15] C. Djurberg, P. Swedlindh, P. Nordblad, M.F. Hansen, F. Bødker, S. Mørup, *Phys. Rev. Lett.* 79 (1997) 5154.
- [16] J.M. Luttinger, L. Tisza, *Phys. Rev.* 70 (1946) 954.
- [17] J.R. Childress, C.L. Chien, J.J. Rhyne, R.W. Erwin, *J. Magn. Magn. Mater.* 104–107 (1992) 1585.
- [18] Y. Ijiri, C.V. Kelly, J.A. Borchers, J.J. Rhyne, D.F. Farrell, S.A. Majetich, *Appl. Phys. Lett.* 86 (2005) 243102.
- [19] D. Farrell, S.A. Majetich, J.P. Wilcoxon, *J. Phys. Chem.* 107 (2003) 11022.
- [20] D.V. Talapin, E.V. Shevchenko, A. Kornowski, N. Gaponik, M. Haase, A.L. Rogach, H. Weller, *Adv. Mater.* 13 (2001) 1868.
- [21] C. Bellouard, I. Mirebeau, M. Hennion, *Phys. Rev. B* 53 (1996) 5770.
- [22] A. Wiedenmann, *Physica B* 297 (2001) 226.
- [23] A. Michels, R.N. Viswanath, J.G. Barker, R. Birringer, J. Weissmuller, *Phys. Rev. Lett.* 91 (2003) 267204.
- [24] J. Weissmuller, A. Michels, J.G. Barker, U. Erb, R.D. Shull, *Phys. Rev. B* 63 (2001) 214414.
- [25] S.L. Lee, T. Thompson, F.Y. Ogrin, C. Oates, M. Wismayer, C. Dewhurst, R. Cubitt, S. Harkness, *Mat. Res. Soc. Symp. Proc.* 803 (2004) GG 4.4.1.
- [26] J. Löffler, G. Kostorz, A. Wiedenmann, W. Wagner, *Physica B* 241–243 (1998) 603.
- [27] J. Löffler, H.-B. Braun, W. Wagner, *Phys. Rev. Lett.* 85 (2000) 1990.
- [28] F. Hellman, A.L. Shapiro, E.N. Abarra, R.A. Robinson, R.P. Hjelm, P.A. Seeger, J.J. Rhyne, J.I. Suzuki, *Phys. Rev. B* 59 (1999) 11408.